ISEIS

Journal of Environmental Informatics 39(1) 67-80 (2022)

Journal of Environmental Informatics

www.iseis.org/jei

Assessing Human Health Risk to DNAPLs Exposure in Bayesian Uncertainty Analysis

Y. Pan[1], X. K. Zeng[1*], X. Y. Gao[1], H. X. Xu[1], Y. Y. Sun[1], D. Wang[1], and J. C. Wu[1]

[1] *Key Laboratory of Surficial Geochemistry, Ministry of Education, School of Earth Sciences and Engineering, Nanjing University, Nanjing 210023, P.R. China*

Received 02 May 2018; revised 10 January 2019; accepted 02 February 2020; published online 13 July 2021

ABSTRACT. The human health risk (HHR) assessment to dense non-aqueous phase liquids (DNAPLs) exposure has become an important part of groundwater environment management. Usually, DNAPL transport models are applied to simulate the concentration distribution of contaminant for HHR assessment. The present paper studied the influences of model uncertainties on the HHR assessment, and the metric of Incremental Lifetime Cancer Risk (ILCR) was used to quantify HHR. The impacts of permeability's heterogeneity and the structure of DNAPL transport model (e.g., the constitutive model) on HHR assessment were evaluated based on a synthetical DNAPL transport model. The results demonstrate that, compared with the low heterogeneity, the high heterogeneity leads to lower average ILCR value at the control planes near the source zone, and higher average ILCR value at the control planes far away from the source zone. In addition, the HHR assessments would be inconsistent for the two constitutive models, i.e., Stone-Parker (S-P) and Corey-van Genuchten (C-v) models. Compared with the HHR assessment depending on C-v model, the mean of ILCR's probability distribution produced by S-P model is larger at the control planes near the source zone, and smaller at the control planes far away from the source zone. Moreover, based on a sandbox experiment, the impact of parameter uncertainty of DNAPL transport model on HHR assessment was evaluated by Markov chain Monte Carlo (MCMC) simulation. The results show that it is infeasible and risky to assess HHR by the specific parameters of contaminant transport model and ignoring parameter uncertainty. The HHR assessment by incorporating Bayesian uncertainty analysis could provide more flexible information. In addition, the sparse grid (SG) surrogate is an effective way to reduce computation burden caused by the larger number of model executions in the MCMC based HHR assessment.

Keywords: human health risk, dense non-aqueous phase liquids, model uncertainty, constitutive models, Markov chain Monte Carlo

1. Introduction

The contamination of groundwater has become a thorny environmental issue threating the ecological system and human health (Aghapour et al., 2018). Dense non-aqueous phase liquids (DNAPLs) are common groundwater contaminants released from the wastewater of electronic and chemical factories, e.g., tetrachloroethene (PCE) (Mccarty et al., 2007; Lin et al., 2018), which cannot dissolve in water with a density exceeding 1 g/cm^3 (Adamson et al., 2003). Due to the complex physical and chemical properties, the removal or remediation of DNAPLs contamination could be difficult and costly (Sabatini et al., 2000). In order to evaluate the potential impact of DNAPLs on human life and provide decisive information for treating contaminated sites, the human health risk assessment to DNAPLs exposure has become a necessary part of groundwater environment management (Christ et al., 2005; Henri et al., 2016).

Human health risk (HHR) assessment refers to the process of evaluating the probability of adverse health effects on humans prone to exposed to contaminated environmental media at present or in the future (EPA, 1989; EPA, 2009). Currently, a commonly used assessment model to quantify HHR is the risk assessment guidance for superfund (RAGS) (EPA, 1989; EPA, 2009). RAGS consists of four parts: hazard identification, dose-response, exposure assessment, and risk characterization (EPA, 1989). In addition, the estimation of exposure assessment is the key step of RAGS. Generally, the result of exposure assessment is described by the average daily dose (ADD) of exposure (EPA, 1989). ADD is influenced by both hydro-geological factors (e.g., contaminant concentration) and behavioral and physiological factors (e.g., exposure duration (ED), exposure frequency (EF)).

Recently, some researches have conducted HHR assessment by detecting contaminant' concentration in groundwater samples from field site. For example, Mishra et al. (2017) applied inductively coupled plasma (ICP) spectrometry to detect contaminants in groundwater samples and evaluate the HHR exposed to various heavy metal contaminants. Fallahzadeh et al. (2018) used inverse distance weighting (IDW) method to identify the spatial and temporal distribution of fluoride contaminant concentrations in Iran and assess HHR for people ranging from 3 to 72 years old. However, it is difficult to obtain contaminant's distribution in groundwater accurately through limited samples. In particular, the distribution of contaminant in groundwater is dynamically changing in time and space.

In recent decades, the numerical/analytical models have been widely used to describe the migration process of contaminant in groundwater when estimating contaminant's concen-

* Corresponding author. Tel.: + 86-025-89680705; fax: + 86-025-83686016
E-mail address: xiankuizeng@nju.edu.cn (X. K. Zeng).

ISSN: 1726-2135 print/1684-8799 online
 doi:10.3808/jei.202100460

tration for HHR assessment (Maxwell et al., 1999; Barros and Rubin, 2008; Siirila and Maxwell, 2012a; Zarlenga et al., 2016). Kumar et al. (2013) established a simple flow and transport model to simulate the residual concentration of pesticide lindane, and the simulated concentration distribution is treated as the input of HHR assessment. However, groundwater is an open and dynamic system, and the transport of contaminants in groundwater is influenced by many factors, e.g., flow rate, aquifer's properties, adsorption, biodegradation.

Modeling uncertainty has been well recognized in groundwater/hydrology community, the outputs of groundwater model could be unreliable due to biased model parameters and model structure. Especially, simulating DNAPLs transport in groundwater is even tougher because DNAPLs could accumulate and form a pool when they are hindered by an aquitard or a lense with low permeability (Emanuel and Sapsford, 2016). Moreover, the DNAPL pools would become the new sources of the contaminant, which makes the simulation of DNAPL transport more complicated (Kueper and Mason, 1996). Due to the driving of these uncertainty factors, the contaminant distributions produced from groundwater model are inevitably eroded with uncertainties. Based on probability statistics theory, the contaminant's concentration can be described in terms of probability density function by taking into account all uncertainty sources (Zeng et al., 2015; Ju et al., 2018).

The heterogeneity of porous media, dispersion, biodegradation and reaction of the contaminants in transport process have been considered as important uncertain sources in HHR assessment (Siirila and Maxwell, 2012b; Barros and Fiori, 2014). Maxwell et al. (1998) assessed the HHR of a drinking water source exposed to PCE by considering both behavioral factors and aquifer parameters uncertainties. They investigated the influence of heterogeneity degree on HHR. Henri et al. (2015, 2016) discussed the influence of different forms of DNAPL, different injection modes and the degradation of chemical mixtures on HHR assessment. They verified the impact of the uncertainty of permeability filed on HHR assessment but did not focus on uncertainty quantification. Moreover, Stewart and Hursthouse (2018) demonstrated that the uncertainties in each step of the assessment framework should be fully considered. Nowadays, various methods have been applied to deal with the uncertainty in HHR assessment, such as fuzzy mathematics (Chen et al., 2017; Dutta, 2017), regression analysis (Mondal et al., 2008), and Markov chain Monte Carlo (MCMC) simulation (Lester et al., 2007; Bernillon and Bois, 2000). Currently, MCMC is mainly applied for quantifying the uncertainty related to toxicity properties in HHR assessment, but seldom employed for treating the uncertainty derived from contaminant transport model. Nevertheless, MCMC has been widely used for the uncertainty quantification of water resources and environment models by integrating the powerful and efficient sampling algorithms (Zhang et al., 2018). This study evaluated the uncertainty of contaminant transport model by incorporating MCMC simulation into HHR assessment.

The permeability of pours media has great impact on groundwater flow field and DNAPL transport (Zheng et al., 2015). DNAPLs would accumulate above the low permeability porous media as pools and transport preferentially through the high permeability areas (Yang et al., 2018). Thus, the media's permeability could contribute important uncertainty to HHR assessment when using DNAPL transport model to generate contaminant's distribution. In order to reduce the uncertainty of transport model, Fernàndez-Garcia et al. (2012) identified 5 model parameters and used one realization of the stochastic permeability field to conduct the risk assessment. However, the heterogeneity of permeability field cannot be represented appropriately by using one realization. Based on a sandbox DNAPL transport experiment, we evaluated the uncertainty of media's permeability to HHR assessment through MCMC simulation, and this is the first focus of this study. In addition, to overcome the heavy computation burden caused by the large number of executions of DNAPL transport model in Bayesian uncertainty analysis, the sparse grid technique was implemented to build surrogate for that DNAPL transport model.

Nowadays many researchers have recognized that model structure can be the important uncertainty source in groundwater/surface water modeling (Refsgaard et al., 2006; Gupta et al., 2012). Due to the lack of the understanding of site conditions and misleading simplification of complex processes, model structure uncertainty is inevitable in DNAPL transport modeling (Thomsen et al., 2016). As a result, the simulated contaminant's concentration distribution could be unreliable because of model structure uncertainty. Koch and Nowak (2015) pointed out that the model structure uncertainty could be partly reduced by setting proper pore-scale, because it can characterize the entire soil and aquifer structure reasonably. However, this is infeasible for large scale groundwater contaminant transport models, e.g., field scale or basin scale. The DNAPL transport in groundwater system can be regarded as a multiphase flow problem, which involves the aqueous phase and DNAPL phase. Generally, the constitutive models are used to describe the important properties (e.g., capillary pressures and relative permeability) of the fluids in porous media. In order to evaluate the impact of model structure uncertainty on HHR assessment, two DNAPL transport constitutive models are used to assess HHR respectively based on a synthetical DNAPL transport model, and this is the second focus of this study.

The innovation of this study is that we evaluated the uncertainties of several important factors (e.g., permeability heterogeneity, constitutive model structure) on DNAPL transport modeling and HHR assessment through Bayesian uncertainty analysis. This paper is organized as follows: the HHR assessment model, DNAPL transport model and MCMC simulation are briefly introduced in Section 2. The implementation details of DNAPL transport models to a synthetical case and a sandbox experiment are described in Section 3. The application of methodologies is described in Section 4. The results and discussions on the influence of model parameter and structure uncertainties on HHR assessment are presented in Section 5. Finally, the summary and discussions of our study are drawn in Section 6.

2. Methodology

2.1. Human Health Risk (HHR) Model

In this study, the HHR assessment is based on RAGS (EPA,

1989), and a commonly used metric - Incremental Lifetime Cancer Risk (ILCR) is used to quantify HHR. Typically, the acceptable risk value of ILCR ranges between 1×10^{-4} and 1×10^{-6}. For ease of illustration, we set the acceptable risk value to 1×10^{-6}, which means that related prevention measures should be taken when ILCR exceeds 1×10^{-6}. ILCR represents the increased probability that one person will have cancer during the lifetime because of the exposure to potential chemical carcinogens (Ogbeide et al., 2016). In this study, we focused on the threats arising from the exposure to a typical DNAPL contaminant tetrachloroethylene (PCE).

ILCR is an integrated metric over time. It can be formally written as (Henri et al., 2016):

$$ILCR = 1 - \exp^{-[ADD \times CPF]} \tag{1}$$

where ILCR is the human health risk, CPF is the metabolized cancer potency factor [kg d/mg], ADD is the average daily dose of the exposure via direct ingestion of PCE [mg/(kg d)], given by EPA (2009):

$$ADD = \langle C \rangle \frac{IR \times ED \times EF}{BW \times AT} \tag{2}$$

where IR is the ingestion rate of water per day [L/d], BW is the common body weight [kg], ED is the exposure duration [y], EF is the daily exposure frequency [d/y], AT is the expected lifetime [d], <C> is the average concentration of PEC during the exposure duration. There are various exposure pathways in reality, such as ingestion of contaminated water, inhalation from polluted air, exposure to contaminant in the skin, and so on. The focus of this work is the transport of DNAPLs from the source zone to the environmental sensitive locations. In order to simplify the issue, only the exposure pathway of ingestion of contaminated water is taken into account. The average concentration <C> in Equation (2) is mathematically expressed by Maxwell and Kastenberg (1999):

$$\langle C \rangle = \max \left\{ \sum_{t}^{t+ED} c(t)/ED \right\} \tag{3}$$

where $c(t)$ is the flux-averaged concentration.

2.2. DNAPL Transport Model

The processes of groundwater flow and DNAPL transport were simulated numerically in this study. DNAPL is a quasi-immiscible fluid and the DNAPL transport is considered as a multiphase flow problem. The movement of each phase (e.g., aqueous phase, DNAPL phase) in multiphase flow can be described by pressure and gravity in a heterogeneous form of Darcy's law (Falta et al., 1995; Pruess et al., 1999). The balance equation for component κ (κ = *w*-water, *a*-air, *n*-DNAPL) over three phases β (β = *g*-gas, *w*-aqueous, *n*-DNAPL) is written as (Falta et al., 1995):

$$\frac{d}{dt}\int_{V_n} \varphi \sum_{\beta} \left(S_\beta \rho_\beta X_\beta^\kappa \right) dV_n = \int_{\Gamma_n} \left[\sum_{\beta} -k \frac{k_{\beta r} \rho_\beta}{\mu_\beta} \left(\nabla p_\beta - \rho_\beta \mathbf{g} \right) \right] \mathbf{n} d\Gamma_n + \int_{V_n} q^\kappa dV_n \tag{4}$$

where t is time [s], φ is the porosity, S_β is the saturation (pore volume fraction) occupied by phase β, ρ_β is the β phase density [kg/m^3], X_β^κ is the mass fraction of component κ in phase β, V_n is arbitrary flow region, Γ_n is surface area [m^2], k is the absolute permeability [m^2], $k_{r\beta}$ is the relative permeability of phase β [m^2], μ_β is the β phase dynamic viscosity [cP], P_β is the fluid pressure in phase β [Pa], g is the gravitational acceleration vector [m/s^2], n is the inward unit normal vector, and q^κ is the rate of heat generation per unit volume. In the Equation (4), the pressure P_β and saturation S_β are defined by capillary pressure function and relative permeability function respectively, and both of them are called constitutive models (Croise et al., 1995).

For multiphase flow simulations, the capillary pressures and relative permeability are important factors that determine the migration and distribution of fluids in a soil-groundwater system (Mathew et al., 2005). In this study, in order to evaluate the impact of constitutive model on the DNAPL transport model based HHR assessment, the Stone model (Stone, 1970) and Corey model (Brooks and Corey, 1964) were used to define relative permeability function respectively. The Parker model (Parker and Lenhard, 1987) and van Genuchten model (van Genuchten, 1980) were used to define capillary pressure functions respectively.

Stone model is a common three phase relative permeability function written as (Stone, 1970):

$$k_{rg} = \left[(S_g - S_{gr}) / (1 - S_{wr}) \right]^n \tag{5}$$

$$k_{rw} = \left[(S_w - S_{wr}) / (1 - S_{wr}) \right]^n \tag{6}$$

$$k_{rn} = \left[\frac{1 - S_g - S_w - S_{nr}}{1 - S_g - S_{wr} - S_{nr}} \right] \left[\frac{1 - S_{wr} - S_{nr}}{1 - S_w - S_{nr}} \right] \left[\frac{\left(1 - S_g - S_{wr} - S_{nr}\right)\left(1 - S_w\right)}{1 - S_{wr}} \right]^n \tag{7}$$

$$S_w + S_g + S_n = 1 \tag{8}$$

where $S_{\beta r}$ is the residual saturation occupied by phase β and n is fitting parameter.

Corey model is a traditional relative permeability function as follows (Brooks and Corey, 1964):

$$k_{rl} = S_*^4 \tag{9}$$

$$k_{rg} = \left(1 - S_*\right)^2 \left(1 - S_*^2\right) \tag{10}$$

$$S_* = \frac{S_l - S_{lr}}{1 - S_{lr} - S_{gr}} \tag{11}$$

Parker model is a frequently-used three phase capillary function given by (Parker and Lenhard, 1987):

$$S_{we} = \frac{S_w - S_m}{1 - S_m} \tag{12}$$

$$S_{le} = \frac{S_w + S_n - S_m}{1 - S_m} \tag{13}$$

$$P_{cgn} = -\frac{\rho_w \mathbf{g}}{\alpha_{gn}}\left[\left(S_{le}\right)^{-\frac{1}{m}} - 1\right]^{\frac{1}{n}} \tag{14}$$

$$P_{cgw} = -\frac{\rho_w \mathbf{g}}{\alpha_{nw}}\left[\left(S_{we}\right)^{-\frac{1}{m}} - 1\right]^{\frac{1}{n}} - \frac{\rho_w \mathbf{g}}{\alpha_{gn}}\left[\left(S_{le}\right)^{-\frac{1}{m}} - 1\right]^{\frac{1}{n}} \tag{15}$$

$$m = 1 - \frac{1}{n} \tag{16}$$

where S_{we} is the effective saturation occupied by phase water, S_{le} is the effective saturation occupied by phase liquid, S_m is the residual saturation occupied by phase liquid, P_{cgn} is gas-DNAPL capillary pressure [Pa], P_{cgw} is gas-water capillary pressure [Pa], α_{gn} is the reciprocal of gas-DNAPL intake pressure, α_{nw} is the reciprocal of DNAPL-water intake pressure, and m is fitting parameter.

Van Genuchten model is one of the foundational capillary and saturation relationships models written as (van Genuchten, 1980):

$$S_{le} = \left[1 + \left(\alpha\beta P_c\right)^n\right]^{-m} \tag{17}$$

where α is fitting parameter, β is a scaling factor, and P_c is capillary pressure [Pa].

The numerical simulator, T2VOC, was applied in this study to simulate DNAPL transport based on the Equations (4) ~ (17). T2VOC uses the integral finite-difference method for spatial discretization and it has been used for many multiphase contamination transport issues (Mccarty and Falta, 1997; Zheng et al., 2015). More details about T2VOC can be found in Falta et al. (1995).

2.3. Markov Chain Monte Carlo Theorem

Considering a nonlinear model (e.g., DNAPL transport model) $M = f(\boldsymbol{\theta})$, the observation data $\mathbf{D}$ is defined as:

$$\mathbf{D} = f(\boldsymbol{\theta}) + \boldsymbol{\varepsilon} \tag{18}$$

where $\boldsymbol{\theta}$ [$\boldsymbol{\theta}_1$, $\boldsymbol{\theta}_2$…, $\boldsymbol{\theta}_d$] represents model parameters, and ε represents residual error derived from measurement error, biased model parameters and model structures. The posterior distribution $p(\boldsymbol{\theta}|\mathbf{D}, M)$ of parameters can be estimated through Bayes' theorem:

$$p(\boldsymbol{\theta}|\mathbf{D}, M) = \frac{p(\mathbf{D}|\boldsymbol{\theta}, M)\,p(\boldsymbol{\theta}|M)}{p(\mathbf{D}|M)} = \frac{p(\mathbf{D}|\boldsymbol{\theta}, M)\,p(\boldsymbol{\theta}|M)}{\int p(\mathbf{D}|\boldsymbol{\theta}, M)\,p(\boldsymbol{\theta}|M)\,d\boldsymbol{\theta}} \tag{19}$$

where p($\boldsymbol{\theta}|M$) is the prior distribution of parameters $\boldsymbol{\theta}$, p($\mathbf{D}|\boldsymbol{\theta}$, M) is the joint likelihood function of parameters $\boldsymbol{\theta}$ and observation data $\mathbf{D}$, which is also denoted as L($\boldsymbol{\theta}|\mathbf{D}$, M), p($\mathbf{D}|M$) is the marginal likelihood of model M, which is a multidimensional integral of joint likelihood in the prior distribution space. In practice, the prior distribution p($\boldsymbol{\theta}|M$) is user-specified according to experts' experience and pilot experiments, and the joint likelihood p($\mathbf{D}|\boldsymbol{\theta}$, M) can be expressed as:

$$L(\theta|\mathrm{D}, M) = \frac{1}{(2\pi)^{n/2}|\mathrm{C}|^{1/2}} \exp\left(-\frac{1}{2}(\mathrm{D} - \boldsymbol{f})^T \mathrm{C}^{-1}(\mathrm{D} - \boldsymbol{f})\right) \tag{20}$$

where C represents residuals' covariance matrix, and n is the number of observations.

It is difficult to obtain the analytical expression of posterior distribution p($\boldsymbol{\theta}|\mathbf{D}$, M) because of the complexity of likelihood function p($\mathbf{D}|\boldsymbol{\theta}$, M). However, Markov chain Monte Carlo (MCMC) method is capable of generating samples from the posterior distribution by constructing Markov chains that satisfy

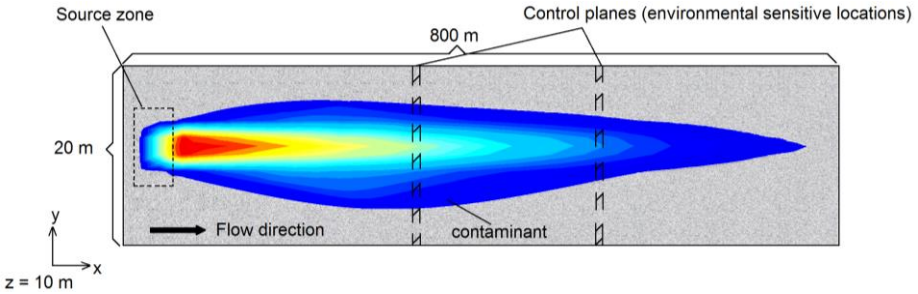

Figure 1. Planform of the DNAPL transport in the synthetical case (the cross section is located at z = 10 m).

ergodicity and reversibility. Then the obtained samples are used to construct p(**θ**|**D**, *M*) by statistical analysis. Differential evolution adaptive Metropolis (DREAMzs) (Vrugt and Ter Braak, 2011; Laloy and Vrugt, 2012) is an effective and robust MCMC sampling algorithm, which integrates differential evolution, sampling randomized subspace sampling, and snooker update techniques, etc. In addition, DREAMzs is designed to solve high-dimensional and multimodal problems, e.g., the likelyhood function of DNAPL transport model. In this study, the saturation of DNAPL is used as observed data **D**.

3. Descriptions to DNAPL Transport Cases

3.1. Synthetical DNAPL Transport Case

A synthetical DANPL transport case was considered by assuming a three-dimensional confined aquifer contaminated by tetrachloroethylene (PCE) that the density is 1620 kg/m^3 and the viscosity is 0.88 cp. The domain was a cuboid with length L_X = 800 m, width L_Y = 20 m, and thickness L_Z = 20 m. Figure 1 showed the planform of the DNAPL transport in the synthetical case. This aquifer had a constant flow boundary condition with inflow at the sites of x = 0 m, and outflow at x = 800 m, and the flowrate was set to 4000 m^3/d. In addition, the other boundaries were all defined as no-flow conditions.

The release of PCE source into this aquifer had stopped prior to the HHR assessment, and 45 kg of PCE remained in the groundwater at the start time of PCE transport model. Thus, this synthetical case focused on the HHR assessment to the transport of remained PCE contamination. In this study, the environmental sensitive locations are represented by control planes x along the longitudinal direction. In the x direction, 40 equally spaced control planes were placed in the model domain to detect the concentration of PCE contamination. We calculate ILCR at different distances from the contaminant source area along the water flow direction.

In this synthetical case study, the aquifer's permeability was assumed as unknown when building DNAPL transport model to simulate contaminant's concentration distribution. A stochastic framework was applied to describe the heterogeneity of this aquifer, and the permeability-filed (k) was considered as a random space function. The detailed description to the structure of k field was given in Section 4.1.

3.2. Sandbox Experiment Case

As shown by Figure 2, a two-dimensional sandbox experiment was conducted to simulate the transport of PCE in heterogeneous porous media (Wu et al., 2017). The sandbox was built with length L_X = 0.6 m, width L_Y = 0.45 m, and thickness L_Z = 0.016 m. The left side of the sandbox was an inflow boundary condition with a constant flowrate of 7.2×10^{-3} m^3/d, which was controlled by a peristaltic pump. In addition, five rectangular lenses with low permeability were placed in the sandbox to simulate the impact of heterogeneity on the transport of PCE.

In this sandbox experiment, the injection point of PCE located at x = 0.3 m, y = 0.4 m, and z = 0.008 m. The PCE saturations in the sandbox were monitored by light transmission method (LTM) (Wu et al., 2018). Moreover, prior to the HHR assessment to PCE transport, the contamination source had stopped leaking into the groundwater system. Thus, this case study focused on the remained contamination in the aquifer. Figure 3 shows the PCE saturation distribution in the sandbox at the start time of HHR assessment.

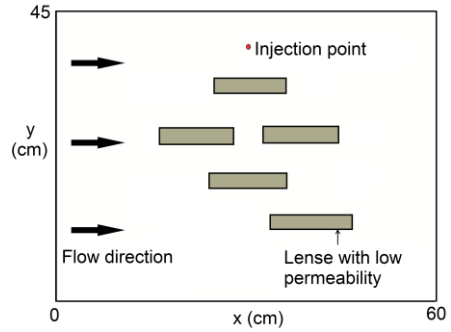

Figure 2. Schematic diagram of the two-dimensional PCE sandbox experiment.

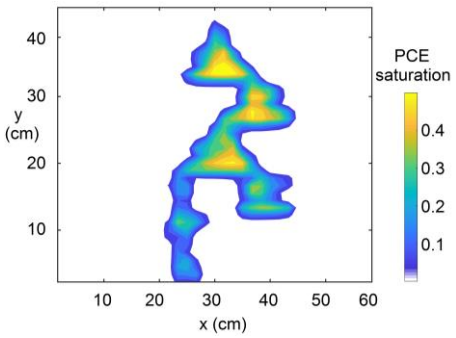

Figure 3. The saturation distribution of PCE at the start time of HHR assessment.

4. Application of Methodology

In the case study of a synthetical DNAPL transport model, the impact of aquifer's heterogeneity and model structure uncertainty (e.g., the constitutive model) on HHR assessment was evaluated. In the case study of a DNAPL transport sandbox experiment, the impact of parameter uncertainty (e.g., the permeability parameters) on HHR assessment was evaluated. Moreover, the sparse grid surrogate technique was used to overcome the heavy computation burden of HHR assessment when using MCMC to calibrate parameter uncertainty.

4.1. Assessing HHR for the Synthetical DNAPL Transport Model

According to the synthetical case described in Section 3.1, the numerical simulation of PCE migration was performed using T2VOC (Falta et al., 1995). The whole aquifer was discretized into 40 cells in x direction, 5 cells in y direction and 5 cells in z direction. The porosity of the aquifer was set to 0.28, and

the Stone-Parker constitutive model is used. Due to the unknown permeability of the aquifer, the log-permeability (lnk) field was assumed as a random space function following multi-Gaussian distribution (Gelhar, 1993; Marsily et al., 2005), which was described by an isotropic exponential covariance model.

Two heterogeneity scenarios were considered in this synthetical case study, and the variance of log-permeability (σ^2) was used to represent the degree of heterogeneity. The low heterogeneity scenario was presented by setting σ^2 to 0.25, and the high heterogeneity scenario was presented by setting σ^2 to 2.25. For the two scenarios, the means of log-permeability (lnk) field were both defined as -18.4 and the integral scales ratios were both 0.15. The random permeability fields were generated using sequential Gaussian simulation in GSLIB program (Deutsch and Journel, 1995). Moreover, for each heterogeneity scenario, 250 random permeability field realizations were generated and then to build DNAPL transport model, respectively.

Table 1. Parameter Setting for Constitutive Models

Parameter	Value
Stone model	
Water residual saturation, S_{wr}	0.1
DNAPL residual saturation, S_{nr}	0.15
Gas residual saturation, S_{gr}	0
Stone model fitted parameter, n	3
Parker model	
Liquid phase residual saturation, S_m	0
Parker model fitted parameter, n	1.84
Reciprocal of gas-DNAPL intake pressure, α_{gn}	10
Reciprocal of DNAPL-water intake pressure, α_{nw}	11
Corey model	
Liquid phase residual saturation, S_{lr}	0.25
Gas residual saturation, S_{gr}	0
van Genuchten	
van Genuchten fitted parameter, λ	0.457
Liquid phase residual saturation, S_{lr}	0
Reciprocal of intake pressure, $1/P_0$	1.76E-03
Max capillary pressure, P_{max}	50000
Liquid phase saturation, S_{ls}	1

Along the *x* direction of study area (Figure 1), 40 equally spaced control planes were set in the model domain to detect contamination's distribution in the aquifer, which was performed by using T2VOC. ILCR are calculated at these control planes. For each heterogeneity scenario, 250 contaminant's concentration distributions at each control plane are generated based on corresponding permeability field realizations. For each concentration distribution at one control plane, the HHR was quantified by computing the ILCR through Equation (1) and Equation (2). Thus, a total of 250 ILCR values were obtained for each control plane. In addition, the parameters of RAGS model (e.g., Equation (1) and Equation (2)) were defined by referring to Henri et al. (2016), e.g., the CPF was set to 0.002 kg•day/mg, IR was 1.5 L/d, BW was 70 kg, ED was 1 year, EF was 30 day /year, and AT was 365 day.

In order to consider the impact of constitutive model structure on HHR assessment, two model structures, the StoneParker (S-P) and Corey-van Genuchten (C-v) models were used as the constitutive models, respectively, and the HHR assessments based on corresponding DNAPL transport model were evaluated and compared. According to the researches of Shi et al. (2011) and Zheng et al. (2015), the parameters and their values used in the constitutive models are listed in Table 1. The variance of lnk field was defined as 0.25 ($\sigma^2 = 0.25$), and 250 random realizations of permeability fields were generated and used for the two constitutive models based HHR assessments, respectively. The process of HHR assessment for different constitutive models is similar to that for different permeability heterogeneities.

4.2. Assessing HHR for the Sandbox Experiment

As shown by Figure 3, the transport of DNAPL is dominated by the characteristics of the background medium and low permeability lenses. We chose the permeability of these two zones (the background media and the lenses with low permeability), as unknown variables (*k*1, *k*2) when building numerical model for this DNAPL transport sandbox experiment.

The sandbox experimental was considered as a two-dimensional DNAPL transport problem, and the numerical simulation was conducted by T2VOC (Falta et al., 1995). The sandbox domain was discretized into 35 cells in *x* direction, 38 cells in *y* direction, and 1 cell in *z* direction. In this sandbox experiment case study, the Stone-Parker constitutive model was used for the PCE transport simulation, and the related parameters were defined at Table 1. In addition, for the MCMC based uncertainty analysis (see section 2.3), the parameters ($\boldsymbol{\theta}$) *k*1 and *k*2 would be identified. The prior distributions of *k*1 and *k*2 were both assumed as uniform, and *k*1 was defined at [1.0×10^{-10}, 20.0×10^{-10}], and *k*2 was defined at [1.0×10^{-11}, 10.0×10^{-11}]. The saturations of PCE during the injection period in the sandbox were used as observations in this Bayesian analysis, and we chose the saturations at 50^{th} minute in the injection period as validation.

The once execution of this DNAPL transport model by T2VOC takes about 75 seconds in a personal computer with eight-core i7-6700 3.40 GHz processors. The MCMC based Bayesian uncertainty analysis requires 90,000 times model executions in this case study. In order to overcome the heavy computation burden caused by the large number of executions of DNAPL transport model, the sparse grid stochastic collection technique (Zeng et al., 2018) was used to build surrogates when assessing HHR. In this case study, two surrogates were built for HHR assessment, the first was the response relationship between model parameters (e.g., *k*1, *k*2) and log-likelihood function ($L(\boldsymbol{\theta}|\mathbf{D}, M)$ in Equation (20)), which was denoted as likelihood surrogate. The second was the response relationship between model parameters (e.g., *k*1, *k*2) and ILCR value, which was denoted as ILCR surrogate. As a result, the likelihood surrogate was used for MCMC simulation when inferring model parameters' posterior distributions, that is to say the likelihood function $L(\boldsymbol{\theta}|\mathbf{D}, M)$ was calculated by using likelihood surrogate instead of using original DNAPL transport model (i.e.,

T2VOC). Correspondingly, based on the inferred parameters' posterior distributions, the ILCR surrogate was used to produce ILCR's probability distribution when assessing HHR.

When building surrogates with spare grid (SG) technique, the maximum SG levels were set to 8 for both two surrogates, and the adaptive SG refinement levels were set to 5. The adaptive error tolerances of the likelihood and ILCR surrogates were defined as 1×10^{-3} and 1×10^{-9}, respectively, because the log-likelihood value always varied from -1500 to -3500, and the ILCR value always varied from 1.0×10^{-5} to 1.4×10^{-5} in this case study. Figure 4 exhibits the complex response surfaces of the likelihood surrogate (plot a) and ILCR surrogate (plot b), respectively.

Building the likelihood surrogate costs a total of 1,427 model executions, which means 1,427 original DNAPL transport model executions were required to build the SG surrogate. Similarly, the construction of the ILCR surrogate model needs a total of 1,537 model executions. However, compared to the number of model executions required by the MCMC based Bayesian uncertainty analysis (e.g., 90,000 model executions in this case study), this cost is acceptable. Figure 5 shows the accuracy of the two surrogates by comparing the results of surrogate and original model, and the model parameters were randomly sampled pled from corresponding prior distributions. Two metrics were used to quantify the performance of SG surrogates, which included root-mean-square error (RMSE) and coefficient of determination (R^2). For the likelihood surrogate, the RMSE is 5.819, and the R^2 between the results of surrogate and original model is larger than 0.999. For the ILCR surrogate, the RMSE is smaller than 0.005, and the R^2 between the results of surrogate and original model is 0.998. Consequently, the two surrogates are deemed to be accurate adequately when they are used to replace the original DNAPL transport model in the Bayesian uncertainty analysis based HHR assessment.

The differential evolution adaptive Metropolis (DREAMzs) algorithm based MCMC simulation was used to estimate the posterior distributions of two model parameters ($k1$ and $k2$). Three parallel Markov chains were used when implementing DREAMzs to search the model parameters' probability space. The length of each chain was set to 30,000, based on Gelman-Rubin statistics (Gelman and Rubin, 1992), the length of burn-in period was set to 10,000, and the rest of 20,000 samples in each chain were used to produce model parameters' posterior distributions. In addition, the likelihood surrogate was used to calculate likelihood values in this MCMC simulation. As a result, 60,000 posterior parameter samples were obtained through this Bayesian uncertainty analysis, and then the HHR assessment is conducted by using ILCR surrogate.

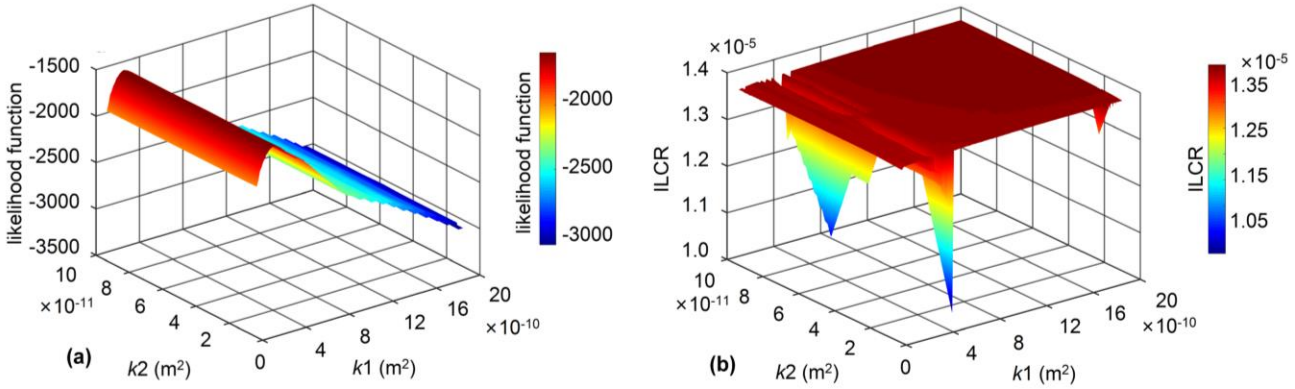

Figure 4. (a) The response surfaces of likelihood surrogate (likelihood function ~ model parameters), (b) The response surfaces of ILCR surrogate (ILCR ~ model parameters).

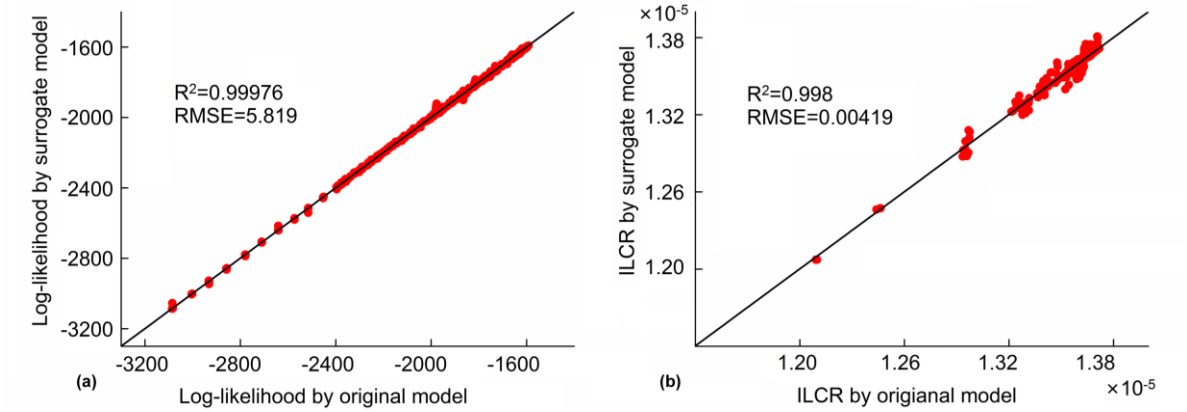

Figure 5. (a) The accuracy performances of likelihood surrogate, (b) The accuracy performances of ILCR surrogate.

5. Results and Discussion

5.1. HHR Assessments of the Synthetical Model

5.1.1. Impact of Aquifer's Heterogeneity on HHR Assessment

ILCR is an integrated metric over time that only relies on position x. Therefore, it could be considered as a temporally integrative risk metric. Figure 6 displays the variation trends of the average ILCRs over 250 k field realizations along the groundwater flow direction profile for $\sigma^2 = 0.25$ and 2.25, respectively. Obviously, the average ILCRs decreases along the flow direction for both two degrees of heterogeneity. In addition, the average ILCRs shows the slight difference for the two heterogeneity scenarios. Along the x direction, compared with the low heterogeneity scenario, the high heterogeneity leads to the lower average ILCR value before the 27th control plane ($\zeta < 27$), and the higher average ILCR after the 27th control plane.

Based on the 250 ILCR samples of each control plane, the ILCR's probability density function (PDF) is produced through frequency analysis for both two heterogeneity scenarios. Figure 7 exhibits the PDF of ILCR at different control planes for $\sigma^2 = 0.25$. Clearly, the mean of ILCR's probability distribution decreases as the control planes being far away from the contaminant source zone, and the maximum mean value of ILCR occurs at the first control plane. Moreover, the mean of ILCR exceeds the acceptable risk value (1×10^{-6}) in front of the 31st ($\xi = 31$) control plane, and necessary contamination treatment measures should be activated. In addition, the probability distribution of ILCR for $\sigma^2 = 2.25$ presents the similar characteristics with that for $\sigma^2 = 0.25$, and so it is not shown in this study.

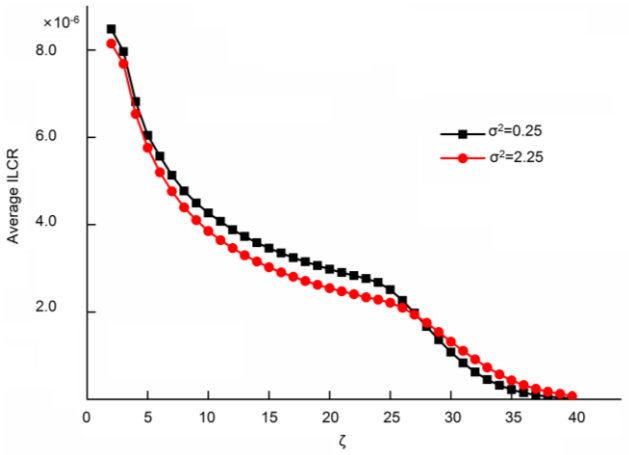

Figure 6. The average ILCR at different control planes (ζ) for $\sigma^2 = 0.25$ and 2.25, respectively.

Figure 8 shows the PDFs of ILCR for two heterogeneity scenarios ($\sigma^2 = 0.25$ and 2.25). The ILCR's probability distribution of high heterogeneity ($\sigma^2 = 2.25$) trends to have a larger variance than that of low heterogeneity ($\sigma^2 = 0.25$). This is because the higher heterogeneity in k field could lead to a higher variability of contaminant's concentration distribution used for HHR assessment. Similar to Figure 6, the mean of ILCR's probability distribution decreases with the distance between control plane and left side ($x = 0$) for both two heterogeneity scenarios. Moreover, the mean of ILCR in the case of high heterogeneity is lower than that of low heterogeneity for the control planes $\zeta < 27$, and then the order of two ILCR's means changes for the control planes $\zeta \geq 27$, which is consistent with the result of Figure 6.

The difference in HHR assessments between the two heterogeneous scenarios could be explained by the principle of preferential flow. The increase of permeability heterogeneity leads to more dominant channels in the aquifer. Contaminant will preferentially pass through these dominant channels for their relatively high permeability. As a result, contaminant can transport further in the aquifer with higher heterogeneity (Zheng et al., 2015). As shown in Figure 9, the two plots (a and b) of first row represent the two realizations of k field with $\sigma^2 = 0.25$, and the second row (c and d) shows the two realizations of k field with $\sigma^2 = 2.25$. It is obviously to find that the porous media with higher heterogeneity (e.g., the plots of c and d) would result in a more complex structure and more dominant channels. Therefore, the higher heterogeneity in aquifer could lead to the higher contaminant concentration, as well as the higher HHR. Moreover, based on the mass balance, the higher concentration in further area means the lower concentration in nearby area. This is the reason for that the high heterogeneity leads to the lower mean of ILCR than low heterogeneity at the position near the source zone ($\zeta < 27$), and the higher mean of ILCR at the position far away from the source zone ($\zeta \geq 27$).

5.1.2. Impact of Constitutive Model on HHR Assessment

Figure 10 shows the PDFs of ILCR calculated by using S-P model and C-v model respectively at different control planes (the σ^2 of k field is 0.25). The two PDFs produced by using different constitutive models have similar shapes. Moreover, in front of the 28th control plane (e.g., $\zeta \leq 28$), the mean of ILCR's PDF produced by using S-P model is larger than that by using C-v model. Correspondingly, after the 28th control plane (e.g., $\zeta > 28$), the probability distribution of ILCR calculated by using S-P model has the smaller mean than that by using C-v model.

The differences between the two constitutive models based HHR assessments are caused by the two reasons that (1) The hysteresis is not considered by C-v model, which is described by S-P model; and (2) C-v model hypothesizes that all the fluids are mobile besides the irreducibly bound wetting phase (Fagerlund et al., 2008). The hysteresis means the different behavior between drainage process and imbibition process, which is described by the capillary pressure - saturation (P_C-S_W) function (Grant and Gerhard, 2007). The hysteresis effect and conditional fluids immobility restrict the advance of wetting front (Lu et al., 1994), and the wetting phase contains contaminant, so the contaminant transport is restricted. Because the hysteresis and conditional immobile fluids are not described by C-v model, the migration of PCE simulated by using C-v model would transport farther than that by using S-P model at the same simulation time. Therefore, the concentration of PCE simulated by using S-P model would be higher than that by using C-v model at the control planes near the contaminant source.

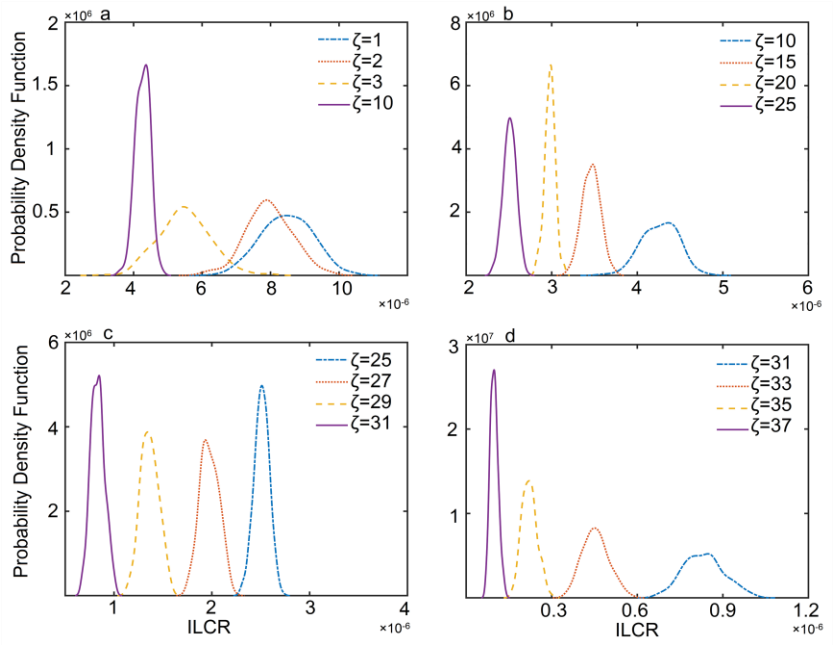

Figure 7. Probability density functions of ILCR at different control planes (ζ) for σ^2 = 0.25. (a) The control planes at ζ = 1, 2, 3, and 10. (b) The control planes at ζ = 10, 15, 20, and 25. (c) The control planes at ζ = 25, 27, 29, and 31. (d) The control planes at ζ = 31, 33, 35, and 37.

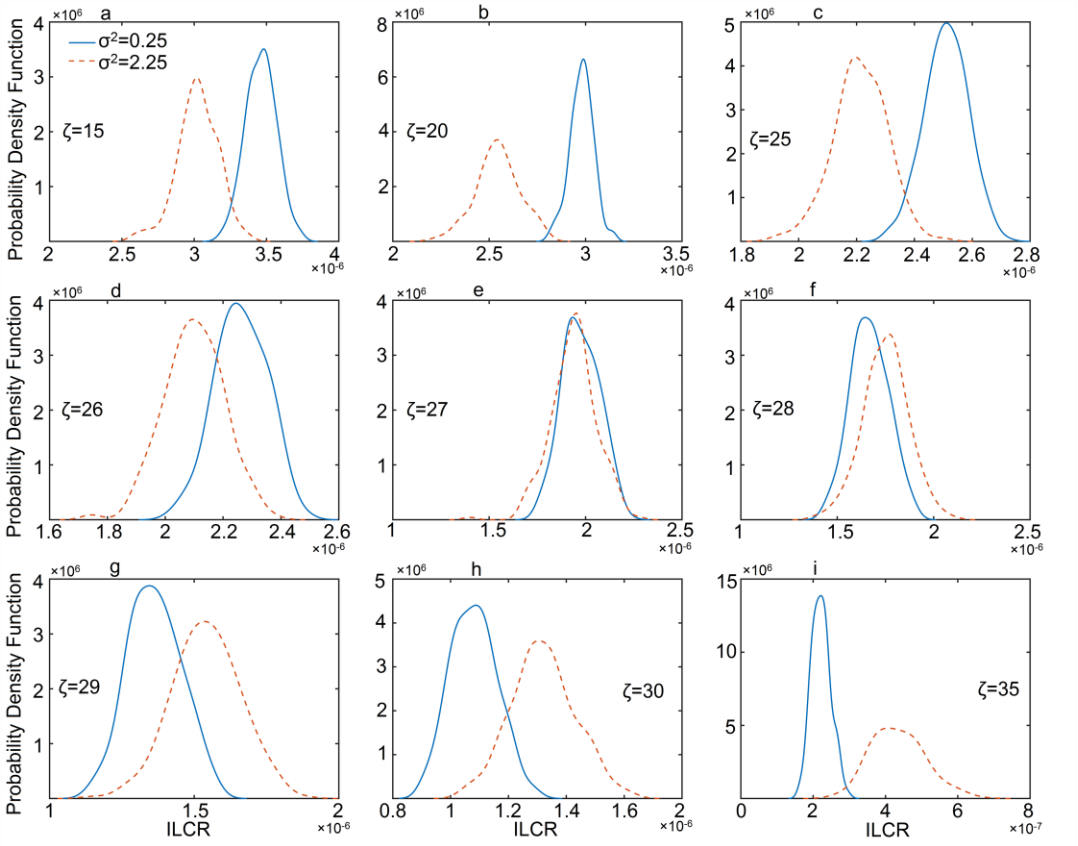

Figure 8. Probability density functions of ILCR for two heterogeneity scenarios (σ^2 = 0.25 and 2.25) respectively at some control planes. (a) ζ = 15. (b) ζ = 20. (c) ζ = 25. (d) ζ = 26. (e) ζ = 27. (f) ζ = 28. (g) ζ = 29. (h) ζ = 30. (i) ζ = 35.

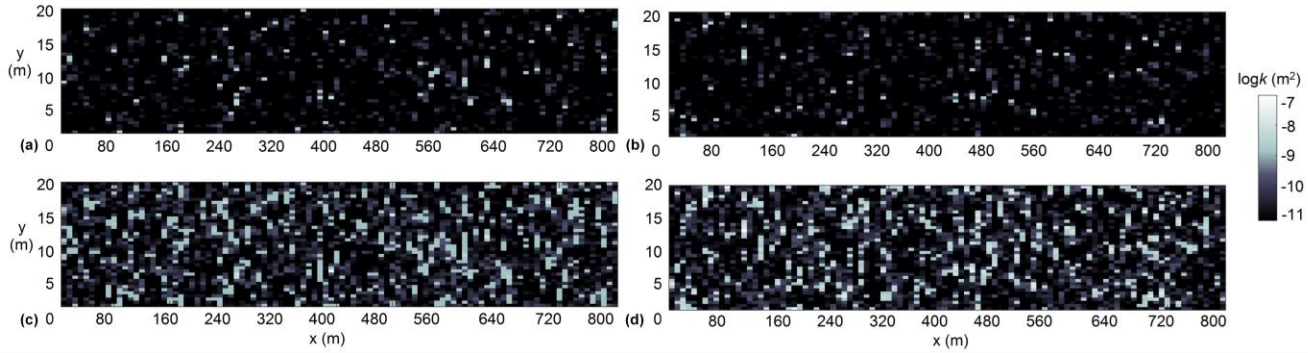

Figure 9. The realizations of k fields with different heterogeneity. (a) and (b) represent the low heterogeneity with $\sigma^2 = 0.25$, (c) and (d) represent the high heterogeneity with $\sigma^2 = 2.25$.

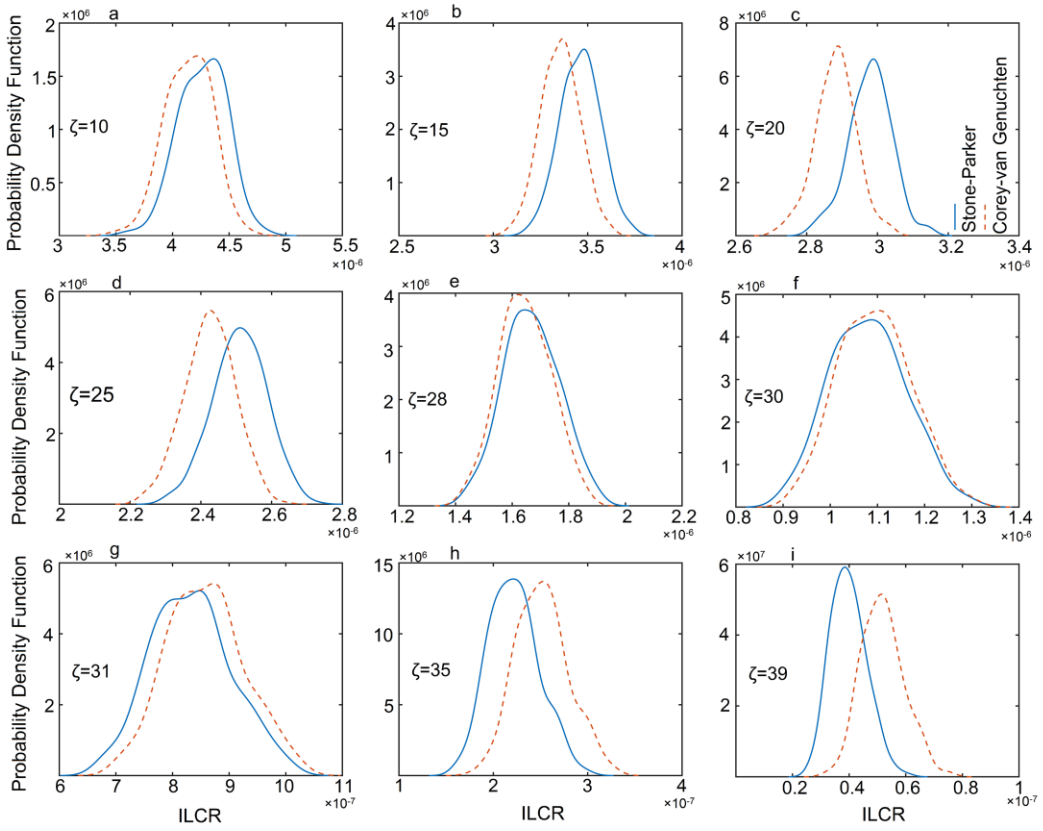

Figure 10. Probability density functions of ILCR for two constitutive models (Stone-Parker and Corey-van Genuchten) respectively at some control planes. (a) $\zeta = 10$. (b) $\zeta = 15$. (c) $\zeta = 20$. (d) $\zeta = 25$. (e) $\zeta = 28$. (f) $\zeta = 30$. (g) $\zeta = 31$. (h) $\zeta = 35$. (i) $\zeta = 39$.

Similarly, the S-P model based PCE simulation would have lower contaminant concentration than the C-v model-based simulation at the control planes far away from source zone. Correspondingly, when calculating ILCR through contaminant's concentration distribution, the HHR assessments would be inconsistent for the two constitutive models.

5.2. HHR Assessments of the Sandbox Experiment

5.2.1. Parameter Uncertainty Based on MCMC Simulation

The frequency distributions of $k1$ and $k2$ were generated based on the obtained posterior samples, as shown in Figure 11. We can find that both two parameters converge to significantly narrower posterior distributions from prior distributions through Bayesian uncertainty analysis. This means that both two parameters were sensitive to the observation (saturation distribution), especially for $k1$. In addition, the posterior distribution of $k1$ shows the characteristics of bimodal distribution, which represents the complexity of parameters' probability space. Thus, it is not easy to determine parameters' empirical values for complex DNAPL transport model.

In order to verify the identified posterior model parame-

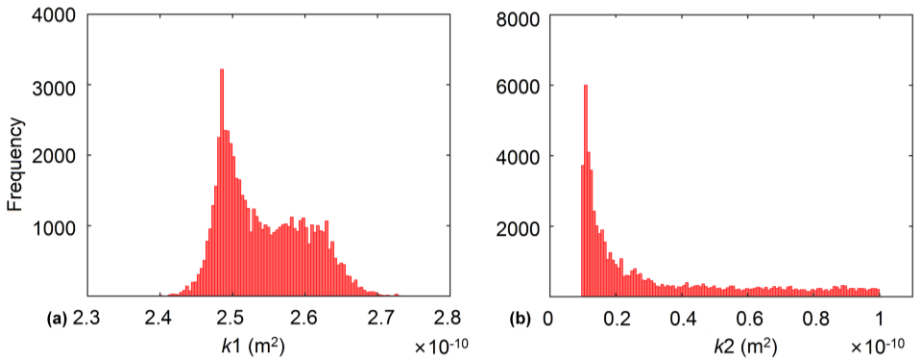

Figure 11. The frequency histograms of model parameters by using the posterior samples of MCMC, (a) represents $k1$ and (b) represents $k2$.

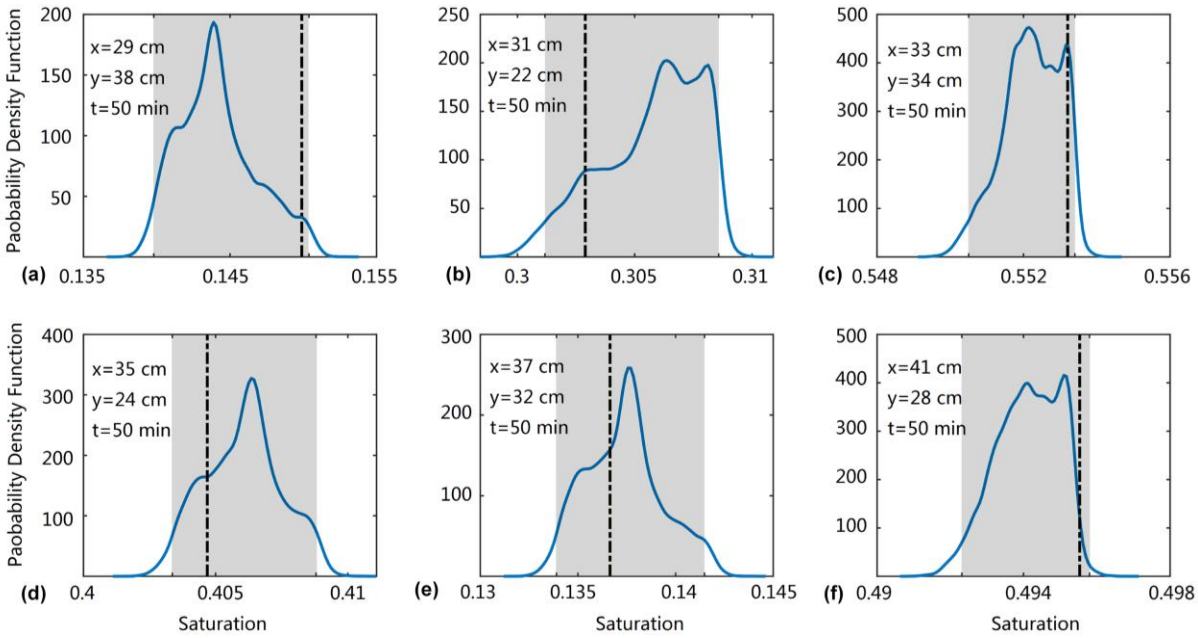

Figure 12. The verifications of the DNAPL transport model, (a) to (f) represent different verification points (The black dash dot line is the observation and the grey zone is the 95% confidence interval).

ters, the obtained posterior predictions are compared with corresponding observations (e.g., saturation). Figure 12 shows the comparison between predictions and observations, and only 6 points in the sandbox domain at the time 50th minute are shown here due to the limitation of paper space. The black dash dot lines mean the observations, and the grey zones represent the 95% confidence intervals of the prediction. It is clearly that all the six observations are included by their 95% confidence intervals, and the predictions at other points have the similar performance and are not shown here. In addition, the predictions obtained by using empirical permeability values, e.g., according to the research of Wu et al. (2018), $k1$ and $k2$ are defined as 1.35×10^{-10} and 3.66×10^{-11}, respectively, are also compared with observations (saturation). Result shows that all predictions obtained by using empirical permeability values are apparently deviated from the observations, e.g., the saturation prediction at x = 29 cm, y = 38 cm is 0.2195 while the observation is 0.1499.

5.2.2. Impact of Parameter Uncertainty on HHR Assessment

Based on the obtained posterior parameter samples, the probability distribution of ILCR was obtained by using ILCR surrogate. As displayed by Figure 13, the distribution of ILCR exhibits apparently characteristics of multimodal distribution. This means that the probability space of ILCR is very complex by incorporating model parameters' uncertainty. By contrast, an empirical ILCR value was calculated by fixing the two model parameters at reference values, e.g., $k1$ was defined as 1.35×10^{-10} and $k2$ was defined as 3.66×10^{-11} (Wu et al., 2018). Correspondingly, the ILCR value was calculated as 1.357×10^{-5}. This value is close to one peak of ILCR's probability distribution, and apparently smaller than the ILCR value with largest probability density. Therefore, it is infeasible and risky to assess HHR to DNAPL exposure by specifying the parameters of contaminant transport model and ignoring parameter uncertainty.

Due to the heavy contamination source of this case study,

the entire probability distribution of ILCR [1.355×10^{-5}, 1.365×10^{-5}] exceeds the acceptable risk value (1×10^{-6}), as well as the empirical ILCR value. In addition, it is possible to search for the "best" model parameters through advanced optimization algorithms, and then assess HHR based on obtained parameter values. However, the Bayesian uncertainty analysis based HHR assessment could provide information that is more flexible for decision makers. We can obtain a credible interval of ILCR at a certain confidence level, for example, under 95% confidence level, the ILCR's credible interval is [1.357×10^{-5}, 1.363×10^{-5}] in this sandbox experiment. In addition, the assessment (e.g., ILCR) based on specific model parameters may underestimate or overestimate the HHR, which may lead to the risk of decision-making failure.

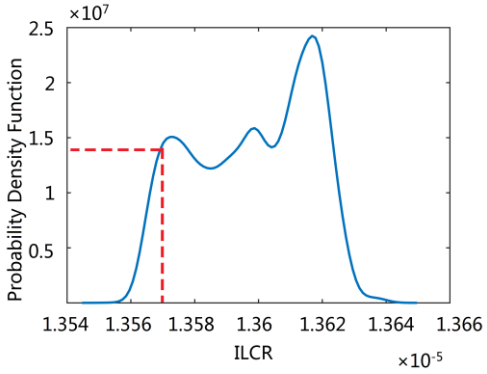

Figure 13. Blue line represents the probability density function of ILCR, and the red dash line represents the ILCR calculated by using empirical parameter values.

6. Summary and Conclusion

Human health risk (HHR) assessment is necessary for the remediation of contaminated site, which is always conducted by building contaminant transport model. The present paper evaluated the influences of model uncertainties on the HHR assessment to DNAPL exposure, and the metric of Incremental Lifetime Cancer Risk (ILCR) was used to quantify HHR. Based on a synthetical DNAPL transport model and a sandbox DNAPL transport experiment, we evaluated the uncertainties of aquifer permeability heterogeneity and constitutive model structure on DNAPL transport modeling and HHR assessment through Bayesian uncertainty analysis. The results from these two case studies could provide insights into the uncertainty quantification and reduction for contaminant transport simulation based HHR assessment under field conditions.

The key findings can be summarized as follows:

(1) Compared with the low heterogeneity in aquifer's permeability field, the high heterogeneity produces lower average ILCR value at the control planes near the source zone, and higher average ILCR value at the control planes far away from the source zone. In addition, for a specific control plane, the ILCR's probability distribution of high heterogeneity has a larger variance than that of low heterogeneity.

(2) The HHR assessments would be inconsistent for the two constitutive models (Stone-Parker and Corey-van Genuchten) because they use different physical mechanisms to describe the transport of DNAPL. Compared with the HHR assessment based on Corey-van Genuchten model, the mean of ILCR's probability distribution produced by using Stone-Parker model is larger at the control planes near the source zone, and smaller at the control planes far away from the source zone.

(3) It is infeasible and risky to assess HHR to DNAPL exposure by specifying the parameters of contaminant transport model and ignoring parameter uncertainty. In addition, the Bayesian uncertainty analysis based HHR assessment could provide more information for decision makers, such as the credible interval of ILCR at a certain confidence level.

(4) The sparse grid (SG) surrogate is an effective way to overcome the problem of computation burden caused by the larger number of model executions in Bayesian uncertainty quantification. Based on SG technique, the likelihood surrogate and ILCR surrogate are built to evaluate the impact of model parameter uncertainty on HHR assessment.

The uncertainties of aquifer heterogeneity and constitutive model structure on DNAPL transport modeling and HHR assessment are evaluated in this study. However, the interactive impact of these factors is not quantitatively analyzed. The Bayesian model averaging (Hoeting et al., 1999; Raftery et al., 2005) or data-driven error model method (Kennedy and O'Hagan, 2001; Xu et al., 2017) provide an effective framework to quantify model parameter and structure uncertainty, and this would be the focus in the subsequent studies. In addition, the behavioral and physiological factors are not considered in this work, the ingestion rate and exposure duration would be considered as important influencing factors in our future study.

Acknowledgments. This study was supported by The National Natural Science Foundation of China (41730856, 41761134089).

References

Adamson, D.T., McDade, M.J., and Hughes, J.B. (2003). Inoculation of a DNAPL source zone to initiate reductive dechlorination of PCE. *Environ. Sci. Technol.*, 2(7882), 2525-2533. http://doi.org/10.1021/es020236y

Aghapour, S., Bina, B., Tarrahi, M.J., Amiri, F., and Ebrahimi, A. (2018). Distribution and health risk assessment of natural fluoride of drinking groundwater resources of Isfahan, Iran, using GIS. *Environ. Monit. Assess*, 190(3), 137. http://doi.org/10.1007/s10661-018-6467-z

Barros, F.P.J.D. and Fiori, A. (2014). First-order based cumulative distribution function for solute concentration in heterogeneous aquifers: Theoretical analysis and implications for human health risk assessment. *Water Resour. Res.*, 50(5), 4018-4037. http://doi.org/10.1002/2013WR015024

Barros, F.P.J.D. and Rubin, Y. (2008). A risk-driven approach for subsurface site characterization. *Water Resour. Res.*, 44(1), 568-569. http://doi.org/10.1029/2007WR006081

Bernillon, P. and Bois, F.Y. (2000). Statistical issues in toxicokinetic modeling: A Bayesian perspective. *Environ, Health Perspect.*, 108(5), 11. http://doi.org/10.2307/3454322

Brooks, R.H. and Corey, A.T. (1964). *Hydraulic Properties of Porous Media*. McGill-Queen's University Press, 352-366.

Chen, J., Qian, H., Wu, H., Gao, Y., and Li, X. (2017). Assessment of arsenic and fluoride pollution in groundwater in Dawukou area, Northwest China, and the associated health risk for inhabitants. *Environ. Earth Sci.*, 76(8), 15. http://dx.doi.org/10.1007/s12665-017-6629-2

Christ, J.A., Ramsburg, C.A., Abriola, L.M., Pennell, K.D., and Löffler, F.E. (2005). Coupling aggressive mass removal with microbial reductive dechlorination for remediation of DNAPL source zones: A review and assessment. *Environ. Health Perspect.*, 113(4), 465-477. http://doi.org/10.1289/ehp.6932

Croise, J., Helmig, R., and Sheta, H. (1995). Numerical simulation of DNAPL-infiltration processes in saturated heterogeneous porous media, *International Conference on Groundwater Quality – Remediation and Protection*, IAHS Publications, Prague, Czech Republic pp. 10.

Deutsch, C.V. and Journel, A.G. (1995). GSLIB. *Geostatistical Software Library and User's guide*, 2nd ed.

Dutta, P. (2017). Modeling of variability and uncertainty in human health risk assessment. *Methodsx*, 4(C), 76-85. http://doi.org/10.1016/j.mex.2017.01.005

Emanuel, D. and Sapsford, D.J. (2016). Fossil rootlet biopores as conduits for contaminant transport through clay horizons: a case study of DNAPL behaviour in Severn alluvium, UK. *Environ. Earth Sci.*, 75(11), 1-12. http://doi.org/10.1007/s12665-016-5756-5

EPA, U.S. (1989). *Risk Assessment Guidance for Superfund (RAGS)* Part A. U.S. EPA , Rep. EPA, Washington DC.

EPA, U.S. (2009). *Risk Assessment Guidance for Superfund Volume I: Human Health Evaluation Manual* (Part F, Supplemental Guidance for Inhalation Risk Assessment). U.S. EPA, Washington DC.

Fagerlund, F., Niemi, A., and Illangasekare, T.H. (2008). Modeling of nonaqueous phase liquid (NAPL) migration in heterogeneous saturated media: Effects of hysteresis and fluid immobility in constitutive relations. *Water Resour. Res.*, 44(3), 893-897. http://doi.org/10.1029/2007WR005974

Fallahzadeh, R.A., Miri, M., Taghavi, M., Gholizadeh, A., Anbarani, R., Hosseini-Bandegharaei, A., Ferrante, M., and Conti, G.O. (2018). Spatial variation and probabilistic risk assessment of exposure to fluoride in drinking water. *Food Chem. Toxicol.*, 113, 8. http://dx.doi.org/10.1016/j.fct.2018.02.001

Falta, R.W., Pruess, K., Finsterle, S., and Battistelli, A. (1995). *T2VOC User's Guide*.

Fernàndez-Garcia, D., Bolster, D., Sanchez-Vila, X., and Tartakovsky, D.M. (2012). A Bayesian approach to integrate temporal data into probabilistic risk analysis of monitored NAPL remediation. *Adv. Water Resour.*, 36(2), 108-120. http://dx.doi.org/10.1016/j.advwatres.2011.07.001

Gelhar, L.W. (1993). Stochastic subsurface hydrology. *Water Resour. Res.*, 22. Prentice-Hall Inc, New Nork, pp. 135S–145S.

Gelman, A. and Rubin, D.B. (1992). Inference from iterative simulation using multiple sequences. *Stat. Sci.*, 7(4), 457-472. https://doi.org/10.1214/ss/1177011136

Grant, G.P. and Gerhard, J.I. (2007). Simulating the dissolution of a complex dense nonaqueous phase liquid source zone: 1. Model to predict interfacial area. *Water Resour. Res*., 43. http://doi/10.1029/2007WR006038

Gupta, H.V., Clark, M.P., Vrugt, J.A., Abramowitz, G., and Ye, M. (2012). Towards a comprehensive assessment of model structural adequacy. *Water Resour. Res*., 48(8), http://doi.org/10.1029/2011WR011044

Henri, C., Fernandezgarcia, D., and De Barros, F. (2015). Probabilistic human health risk assessment of chemical mixtures: hydrotoxicological interactions and controlling factors. *Water Resour. Res*., 4086-4108. http://doi.org/10.1002/ 2014WR016717

Henri, C.V., Fernàndezgarcia, D., and De Barros, F.P.J. (2016). Assessing the joint impact of DNAPL source-zone behavior and degradation products on the probabilistic characterization of human health risk. Adv. *Water Resour*., 88, 124-138. http://doi.org/10.1016/j.advwatres.2015.12.012

Hoeting, J.A., Madigan, D., Raftery, A.E., and Volinsky, C.T. (1999). Bayesian model averaging: A tutorial. Stat. Sci. 14(4), 382-401. https://doi.org/10.1214/ss/1009212519

Ju, L., Zhang, J.J., Long, M., Wu, L.S., and Zeng, L.Z. (2018). An adaptive Gaussian process-based iterative ensemble smoother for data assimilation. Adv. *Water Resour.*, 115, 125-135. https://doi.org/10.1016/j.advwatres.2018.03.010

Kennedy, M.C. and O'Hagan, A. (2001). Bayesian calibration of computer models. *J. Roy. Stat. Soc*., B 63, 425-450. http://doi.org/10.1111/1467-9868.00294

Koch, J. and Nowak, W. (2015). Predicting DNAPL mass discharge and contaminated site longevity probabilities: Conceptual model and high-resolution stochastic simulation. *Water Resour. Res*., 51(2), 806-831. http:// doi.org/doi:10.1002/2014WR015478

Kueper, B.H. and Mason, A.R. (1996). Surfactant Enhanced Dissolution of Pooled DNAPL: Numerical Modelling and Parameter Identification, *International Symposium on Groundwater and Subsurface Remediation - Research Strategies for In-situ Technologies Springer Berlin Heidelberg*, Univ Stuttgart, Stuttgart, Germany.

Kumar, V., Barros, F.P., Schuhmacher, M., Fernàndez-Garcia, D., and Sanchez-Vila, X. (2013). Dynamic interactions between hydro - geological and exposure parameters in daily dose prediction under uncertainty and temporal variability. *J. Hazard. Mater*., 263, 197-206. http://doi.org/10.1016/j.jhazmat.2013.08.036

Laloy, E. and Vrugt, J.A. (2012). High-dimensional posterior exploration of hydrologic models using multiple-try DREAM(ZS) and high-performance computing. *Water Resour. Res*., 50(3), 182-205. http://doi.org/10.1029/2011WR010608

Lester, R.R., Green, L.C., and Linkov, I. (2007). Site-specific applications of probabilistic health risk assessment: Review of the literature since 2000. *Risk Anal*., 27(3), 635-658. http://doi.org/10.1111/j.1539-6924.2007.00890.

Lin, K.S., Mdlovu, N.V., Chen, C.Y., Chiang, C.L., and Dehvari, K. (2018). Degradation of TCE, PCE, and 1,2–DCE DNAPLs in contaminated groundwater using polyethylenimine-modified zero-valent iron nanoparticles. *J. Clean Prod*., 175, 456-466. http://doi.org/10.1016/j.jclepro.2017.12.074

Lu, T.X., Biggar, J.W., and Nielsen, D.R. (1994). Water movement in glass bead porous media: 1. Experiments of capillary rise and hysteresis. *Water Resour. Res*., 30(12), 7. http://doi.org/10.1029/97WR00997

Marsily, G.D., Delay, F., Gonçalvès, J., Renard, P., Teles, V., and Violette, S. (2005). Dealing with spatial heterogeneity. *Hydrogeol. J*., 13(1), 161-183. http://dx.doi.org/10.1007/s10040-004-0432-3

Mathew, M., Illangasekare, T.H., Fagerlund, F., and Niemi, A. (2005). *Sensitivity of Model Parameter in the Predication of DNAPL Infiltration and Redistribution in Heterogeneous Porous Media*, American Geophysical Union, Fall Meeting 2005, U.S.A., pp. 105-117.

Maxwell, R.M. and Kastenberg, W.E. (1999). Stochastic environmental risk analysis: an integrated methodology for predicting cancer risk from contaminated groundwater. Stoch. *Environ. Res. Risk Assess*., 13(1-2), 27-47. http://doi.org/10.1007/s004770050030

Maxwell, R.M., Kastenberg, W.E., and Rubin, Y. (1999). A methodology to integrate site characterization information into groundwater-driven health risk assessment. *Water Resour. Res*., 35(35), 2841-2856. http://doi.org/10.1029/1999WR900103

Maxwell, R.M., Pelmulder, S.D., Tompson, A.F.B., and Kastenberg, W.E. (1998). On the development of a new methodology for groundwater-driven health risk assessment. *Water Resour. Res*., 34(34), 833-847. http://doi.org/10.1029/97WR03605

Mccarty, J.L. and Falta, R.W. (1997). Numerical simulation of air sparging for remediation of NAPL contamination. *Groundwater*, 35(1), 12. http://doi.org/10.1111/j.1745-6584.1997.tb00065.x

Mccarty, P.L., Chu, M.Y., and Kitanidis, P.K. (2007). Electron donor and pH relationships for biologically enhanced dissolution of chlorinated solvent DNAPL in groundwater. *Eur. J. Soil Biol*. 43(5-6), 276-282. http://doi.org/10.1016/j.ejsobi.2007.03.004

Mishra, H., Karmakar, S., Kumar, R., and Singh, J. (2017). A framework for assessing uncertainty associated with human health risks from MSW landfill leachate contamination. *Risk Anal*., 37(7), 19. http://doi.org/10.1111/risa.12713

Mondal, D., Hegan, A., Rodriguezlado, L., Banerjee, M., Giri, A.K., and Polya, D.A. (2008). Multiple regression analysis of As groundwater hazard and assessment of As-attributable human health risks in Chakdha Block, *West Bengal. Mineral. Mag*., 72(1), 461-465. http://doi.org/10.1180/minmag.2008.072.1.461

Ogbeide, O., Tongo, I., and Ezemonye, L. (2016). Assessing the distribution and human health risk of organochlorine pesticide residues in sediments from selected rivers. *Chemosphere*, 144, 8. http://doi.org/10.1016/j.chemosphere.2015.09.108

Parker, J.C. and Lenhard, R.J. (1987). A model for hysteretic constitutive relations governing multiphase flow: 1. Saturation-pressure relations. *Water Resour. Res*., 23(12), 2187-2196. http://doi.org/10.1029/WR023i012p02187

Pruess, K., Oldenburg, C.M., and Moridis, G.J. (1999). *TOUGH2 User's Guide Version 2 - eScholarship*, Earth Sciences Division, Lawrence Berkeley National Laboratory, California.

Raftery, A.E., Gneiting, T., Balabdaoui, F., and Polakowski, M. (2005). Using Bayesian Model Averaging to Calibrate Forecast Ensembles. *Mon. Weather Rev*., 133(5), 1155-1174. http://doi.org/ 10.1175/mwr 2906.1

Refsgaard, J.C., Sluijs, J.P.V.D., Brown, J., and Keur, P.V.D. (2006). A framework for dealing with uncertainty due to model structure error. *Adv. Water Resour*., 29(11), 1586-1597. http://doi.org/10.1016/j.advwatres. 2005.11.013

Sabatini, D.A., Knox, R.C., Harwell, J.H., and Wu, B. (2000). Integrated design of surfactant enhanced DNAPL remediation: efficient supersolubilization and gradient systems. *J. Contam. Hydrol.*, 45(1–2), 99-121. http://doi.org/10.1016/S0169-7722(00) 00121-2

Shi, X.Q., Wu, J.C., Liu, D.P., Jiang, S.M., Sun, Y.Y., and Xu, H.X. (2011). Numerical simulation of transportation of dense nonaqueous phase liquids in the subsurface environment. *J. Nanjing Univ*., 47(3), 299-307. http://doi.org/10.13232/j.cnki.jnju. 2011.03.013

Siirila, E.R. and Maxwell, R.M. (2012a). Evaluating effective reaction rates of kinetically driven solutes in large-scale, statistically anisotropic media: Human health risk implications. *Water Resour. Res*., 48(4), 1427-1434. http://doi.org/10.1029/2011WR011516

Siirila, E.R. and Maxwell, R.M. (2012b). A new perspective on human health risk assessment: development of a time dependent methodology and the effect of varying exposure durations. *Sci. Total Environ*., 431(5), 221-232. http://doi.org/10.1016/j.scitotenv. 2012.05.030

Stewart, A. and Hursthouse, A. (2018). Environment and human health: The challenge of uncertainty in risk assessment. *Geosci*., 8(1), 20. http://doi.org/10.3390/geosciences8010024

Stone, H.L., 1970. Probability Model for Estimating Three-Phase Relative Permeability. *J. Pet. Technol*. 22(02), 214-218. http://doi.org/10.2118/2116-PA

Thomsen, N.I., Binning, P.J., Mcknight, U.S., Tuxen, N., Bjerg, P.L., and Troldborg, M. (2016). A Bayesian belief network approach for assessing uncertainty in conceptual site models at contaminated sites. *J. Contam. Hydrol*., 188, 17. http://doi.org/10.1016/j.jconhyd. 2016.02.003

Van Genuchten, M.T. (1980). A closed-form equation for predicting the hydraulic conductivity of unsaturated soils. *Soil Sci. Soc. Am. J*., 44, 9. http://doi.org/10.2136/sssaj1980.03615995004400050002

Vrugt, J.A. and Ter Braak, C.J.F. (2011). DREAM(D): An adaptive Markov Chain Monte Carlo simulation algorithm to solve discrete, noncontinuous, and combinatorial posterior parameter estimation problems. *Hydro. Earth System Sci*., 15(12), 13. http://doi.org/10.5194/hess-15-3701-2011

Wu, M., Wu, J., and Wu, J. (2017). Simulation of DNAPL migration in heterogeneous translucent porous media based on estimation of representative elementary volume. *J. Hydrol*., 553. http://doi.org/10.1016/j.jhydrol.2017.08.005

Wu, M., Wu, J., Wu, J., and Hu, B.X. (2018). A three-dimensional model for quantification of the representative elementary volume of tortuosity in granular porous media. *J. Hydrol*., 557, 128-136. http://doi.org/10.1016/j.jhydrol.2017.12.030

Xu, T.F., Valocchi, A.J., Ye, M., and Liang, F. (2017). Quantifying model structural error: Efficient Bayesian calibration of a regional groundwater flow model using surrogates and a data-driven error model. *Water Resour. Res*., 53(5), 4084-4105. http://doi.org/10.1002/2016WR019831.

Yang, L., Wang, X., Mendoza-Sanchez, I., and Abriola, L.M. (2018). Modeling the influence of coupled mass transfer processes on mass flux downgradient of heterogeneous DNAPL source zones. *J. Contam. Hydrol*., 211, 14. http://doi.org/10.1016/j.jconhyd.2018. 02. 003

Zarlenga, A., Barros, F.P.J.D., and Fiori, A. (2016). Uncertainty quantifycation of adverse human health effects from continuously released contaminant sources in groundwater systems. *J. Hydrol*., 541, 850-861. http://doi.org/10.1016/j.jhydrol. 2016.07.044

Zeng, X., Ye, M., Wu, J., Wang, D., and Zhu, X. (2018). Improved nested sampling and surrogate-enabled comparison with other marginal likelihood estimators. *Water Resour. Res*., 54(2), 30. http://doi.org/10.1002/2017WR020782

Zeng, X., Wang, D., Wu, J.C. (2015). Evaluating the three methods of goodness of fit testfor frequency analysis. *J. Risk Anal*., Crisis Response 5, 178-187. http://doi.org/10.2991/jrarc.2015.5.3.5

Zhang, L.E., Huang, D., Yang, J., Wei, X., Qin, J., Ou, S., Zhang, Z., and Zou, Y. (2017). Probabilistic risk assessment of Chinese residents' exposure to fluoride in improved drinking water in endemic fluorosis areas. *Environ. Pollut*., 222, 118-125. http://doi.org/10.1016/j.envpol. 2016.12.074

Zheng, F., Gao, Y., Sun, Y., Shi, X., Xu, H., and Wu, J. (2015). Influence of flow velocity and spatial heterogeneity on DNAPL migration in porous media: Insights from laboratory experiments and numerical modelling. *Hydrogeol. J*., 23(8), 1703-1718. http://doi.org/10.1007/s10040-015-1314-6